ARTICLES

Journal of Semiconductors
(2023) 44, 082001
doi: 10.1088/1674-4926/44/8/082001

Pressure manipulation of ultrafast carrier dynamics in monolayer WS_2

Yao Li[1], Haiou Zhu[1, 2], and Zongpeng Song[2, †]

[1]New Materials and New Energies, Shen Zhen Technology University, Shenzhen 518118, China

[2]Analysis and Testing Center, Shen Zhen Technology University, Shenzhen 518118, China

Abstract: Two-dimensional transition metal dichalcogenides (TMDs) have intriguing physic properties and offer an exciting platform to explore many features that are important for future devices. In this work, we synthesized monolayer WS_2 as an example to study the optical response with hydrostatic pressure. The Raman results show a continuous tuning of the lattice vibrations that is induced by hydrostatic pressure. We further demonstrate an efficient pressure-induced change of the band structure and carrier dynamics via transient absorption measurements. We found that two time constants can be attributed to the capture process of two kinds of defect states, with the pressure increasing from 0.55 GPa to 2.91 GPa, both of capture processes were accelerated, and there is an inflection point within the pressure range of 1.56 GPa to 1.89 GPa. Our findings provide valuable information for the design of future optoelectronic devices.

Key words: two-dimensional transition metal dichalcogenides; hydrostatic pressure; carrier dynamics; band structure; ultrafast spectroscopy

Citation: Y Li, H O Zhu, and Z P Song, Pressure manipulation of ultrafast carrier dynamics in monolayer WS_2[J]. *J. Semicond.*, 2023, 44(8), 082001. https://doi.org/10.1088/1674-4926/44/8/082001

1. Introduction

Two-dimensional transition metal dichalcogenides (TMDs) have rich electrical, optical, chemical properties, and their bandwidth ranges from visible to infrared. Owing to the excellent mechanical, optical, and electrical properties, TMDs are suitable materials for sensors, catalysts, storage batteries, optoelectronic devices, and excitonic devices[1–4]. Monolayer WS_2 is an atomically thin two-dimensional material, which is a sandwich structure, and is composed of a single layer transition metal tungsten (W) and two layers of chalcogen (S)[5, 6].

One key issue in harnessing novel properties of TMDs is to understand and control the carrier dynamic processes. Because the performance of TMDs-based photoelectric devices are closely related to the carrier dynamics process, effective and continuous tuning of carrier dynamics in TMDs is highly desired. Hydrostatic pressure is pure and clean because no additional impurities are introduced by the hydrostatic pressure of the diamond anvil cell (DAC). Recent reports have indicated that the optoelectronic properties of TMDs can be effectively tuned via hydrostatic pressure, such as the interaction of interlayer, material structure, carrier density, and conductivity[7–13]. The semiconductor to metallic phase transition in bulk WS_2 is caused by hydrostatic pressure[14, 15]. In contrast, there are few studies on the carrier recombination of monolayer TMDs under pressure. Thus, it is of great value to develop an understanding of the carrier dynamics in TMDs with pressure.

Here, monolayer WS_2 is used as a sample to study the carrier dynamics via transient absorption measurements. Our results demonstrate a pressure-induced blue shift of the A-exciton resonance, and two kinds of carrier capture processes of defect states can be continuously tuned by hydrostatic pressure. This study provides basic information for understanding the dynamics of carrier in TMDs, which may be useful in the design of new photoelectric devices that are based on TMDs.

2. Synthesis and material characterization

The WS_2 monolayers were grown by CVD technique at 800 °C for 20 min onto SiO_2/Si, as shown in Fig. 1. Sulfur powder and tungsten trioxide powder with a purity of 99.9% were used as source materials for experimental preparation of samples. Meanwhile, 0.2-g sulfur powder was placed on the crucible in the first temperature zone, and 0.1-g tungsten trioxide powder was placed on the crucible in the second temperature zone. Furthermore, 40 sccm (cubic centimeters per minute) Ar and 5 sccm H_2 was used as the carrier gas to transfer the evaporated sulfur vapor to the substrate. We raised the temperature of furnace 1 from 25 °C to 200 °C for 1 h, and the temperature of furnace 2 from 25 °C to 800 °C, and maintained the temperature for 20 min. The S powder is gasified in the low temperature area, transported to the high temperature area by the carrier gas, and reacts with the gasi-

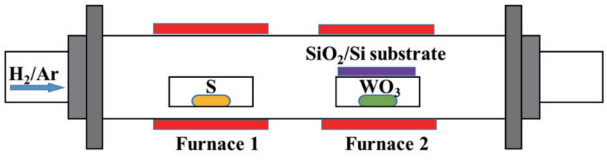

Fig. 1. (Color online) Experimental setup of the CVD growth of monolayer WS_2 sample.

Correspondence to: Z P Song, songzongpeng@sztu.edu.cn
Received 27 FEBRUARY 2023; Revised 27 MARCH 2023.

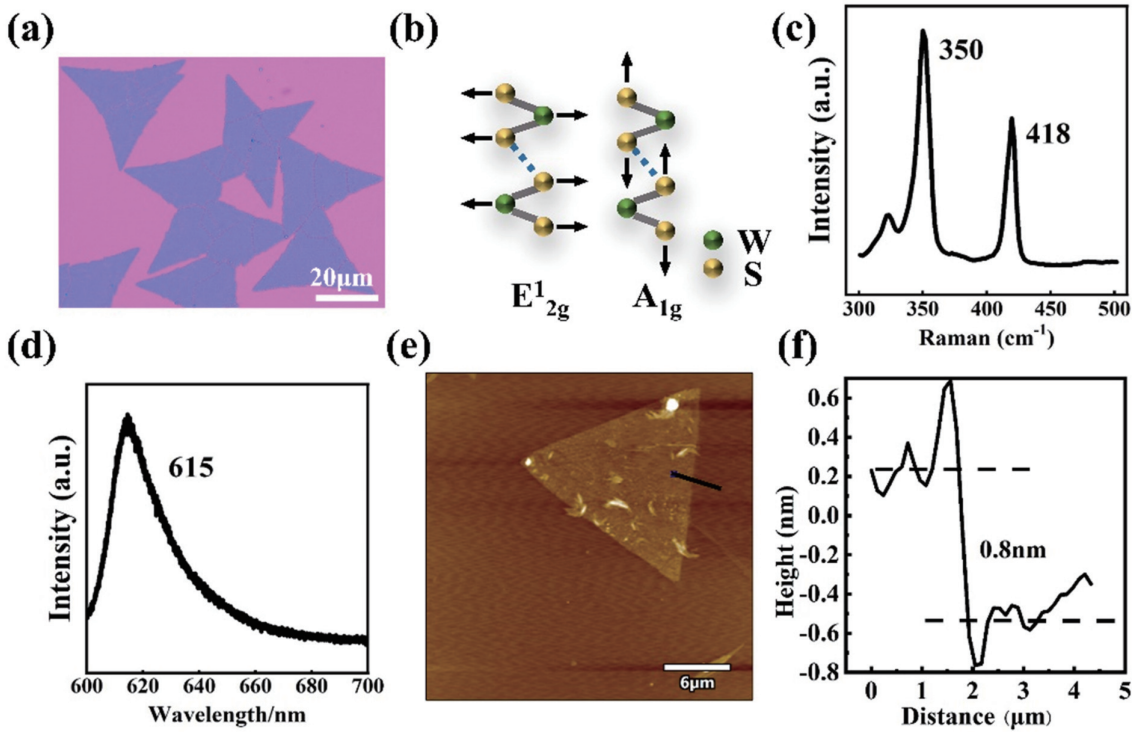

Fig. 2. (Color online) The characterization of monolayer WS_2. (a) Optical image of a monolayer WS_2. (b) Schematics of Raman modes of $E_{2g}{}^1$ and A_{1g}. (c) Raman spectra of monolayer WS_2 sample. (d) PL spectra of monolayer WS_2 sample. (e) AFM image of monolayer WS_2 sample. (f) Height image intensity profile along the black line in (e).

fied WO_3 on the substrate to generate WS_2. The whole CVD equipment was then naturally cooled down to room temperature.

The size of the sample prepared by CVD method can reach 40 μm, as shown in Fig. 2(a). The Raman spectra and photoluminescence (PL) spectra of the sample are shown in Figs. 2(c) and 2(d), respectively. The PL peak of the sample is centered at 615 nm. The Raman peaks of the sample is centered at 350 cm^{-1} and 418 cm^{-1}, which represents the $E_{2g}{}^1$ and A_{1g} peaks of WS_2, respectively. The difference between the $E_{2g}{}^1$ and A_{1g} peaks is 68 cm^{-1}, which is in accord with the characteristics of single layer WS_2[16]. The schematics of these two Raman modes E^1_{2g} and A_{1g} are shown in Fig. 2(b), the A_{1g} mode of monolayer WS_2 originates from the transverse out-of-plane relative vibration between sulfur atoms in the interlayer, while the E^1_{2g} mode originates from the in-plane longitudinal vibration of tungsten and sulfur atoms in opposite directions. Therefore, E^1_{2g} mode vibration is sensitive to the length of W–S bond. The PL peak of the monolayer WS_2 lies at 615 nm (2.02 eV), which indicates that the valence band top and the conduction band bottom of the monolayer WS_2 are located at the transition point, which is a direct bandgap[11]. The AFM image show that the thickness of our monolayer WS_2 sample is 0.8 nm, which is shown in Fig. 2(e) and Fig. 2(f).

The monolayer WS_2 was peeled from the substrate with the PVP/PVA adsorption transfer method. The pressure device used in this experiment is a four-column DAC, and the size of diamond plane is 300 μm. The T301 gasket was prepressed to 50 μm, and a hole with a diameter of 100 μm was punched in the center with a laser. Silicone oil was chosen as a pressure transmission medium. The silicone oil, the monolayer WS_2 sample, and a 10 μm ruby were placed in the hole. The DAC device was used to gradually increase the pressure of the monolayer WS_2 heterostructure to 2.91 GPa from 0 GPa, and the direction in which the pressure applied is perpendicular to the plane of the monolayer WS_2 sample.

3. Results and discussion

Raman measurements were performed to study the lattice vibration of the monolayer WS_2 sample when pressurized in the DAC[17] and the pressure transmission medium (PTM) is silicone oil. The evolutions of Raman spectra show a clear pressure-induced changeover, the feature at 350 cm^{-1} and 418 cm^{-1} (E^1_{2g} and A_{1g} modes of monolayer WS_2) blue shift as the pressure increases (as shown in Fig. 3(a)), which is similar to other layered materials[18, 19]. The Raman peak as a function of pressure is shown in Fig. 3(b), and there are two linear increases at a rate of 3.1 $cm^{-1}GPa^{-1}$ (A_{1g}) and 1.8 $cm^{-1}GPa^{-1}$ (E^1_{2g}), respectively. The A_{1g} modes are more sensitive to pressure than that of the E^1_{2g} modes, which may be the reason why the out-of-plane motion of S–S bonds of A_{1g} modes is more sensitive than the in-plane motion of the W–S bonds of the E^1_{2g} modes under pressure. Therefore, the out-of-plane compression is more favorable than in plane compression under pressure[20, 21].

The PL spectra of monolayer WS_2 with different pressures were measured, as shown in Fig. 4(a). The PL peaks have a blue shift with an increase in pressure from 0 GPa to 2.91 GPa. The PL peaks as a function of pressure are shown in Fig. 4(b), and there is a linear increase at a rate of −2.1 $nm^{-1}GPa^{-1}$. The change of the bandgap can be attributed to the enhanced quantum confinement effect caused by the pressure.

The transient absorption (TA) spectra of monolayer WS_2 with different pressures were measured to gain more insight

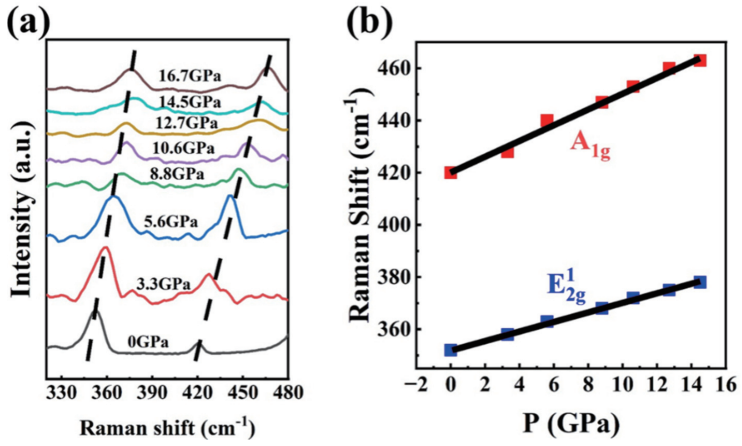

Fig. 3. (Color online) Pressure-induced Raman vibration in monolayer WS_2. (a) Evolution of the Raman spectrum with pressure for monolayer WS_2 sample. (b) Raman vibrations of monolayer WS_2 as a function of pressure.

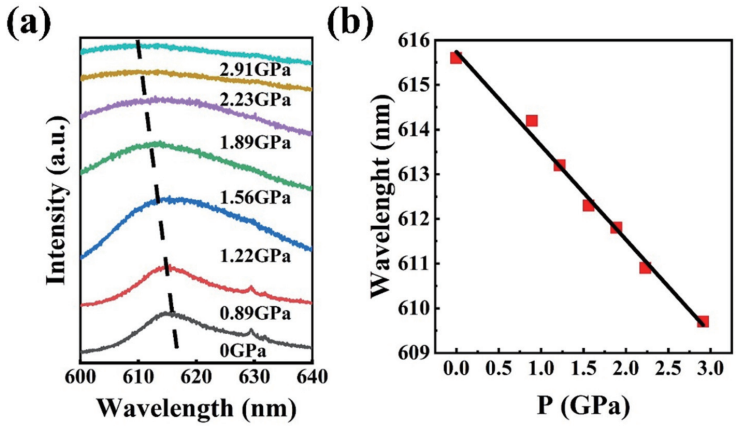

Fig. 4. (Color online) (a) Evolution of the PL spectra of monolayer WS_2 sample with pressures. (b) PL peaks of monolayer WS_2 as a function of pressure.

of the carrier dynamics process (as shown in Fig. 5(a)). For monolayer WS_2, the applied pump wavelength is 400 nm and the pump peak fluence is 10 μJ/cm^2. All of the samples were measured at room temperature.

The absorption peaks of monolayered WS_2 lies at 605–615 nm, which can be assigned to the A exciton resonance of WS_2, and the photo-induced bleaching signals indicate that the corresponding energy states are occupied by photo-induced carriers. The TA spectra traces of A excitons are shown in Fig. 5(b) as the pressure ranged from 0.55 to 2.91 GPa at a time delay of 3 ps. A blue shift of the A exciton and the decrease of the intensity is observed with the increase of pressure. As shown in Fig. 5(c), the peaks of photo-induced signals with different pressures can be linearly fitted with a slope of −5.93 nm/GPa. These features might be caused by the pressure-induced enlargement of the bandgap of TMDs[22–25].

The representative TA signals of A excitons with different pressures were recorded, as shown in Fig. 6. The decay curve can be well fitted as $\Delta A = A_1 e^{-\tau_1} + A_2 e^{-\tau_2}$ with two time constants. Because the vacancies of atoms and grain boundary dislocations are common in TMDs, the capture process of shallow and deep defects states may give rise to the time constants τ_1 and τ_2[26–28].

It should be noted that the carrier capture process gets faster when increasing the pressure from 0.55 to 2.91 GPa, and can be divided into two distinct regions according to the

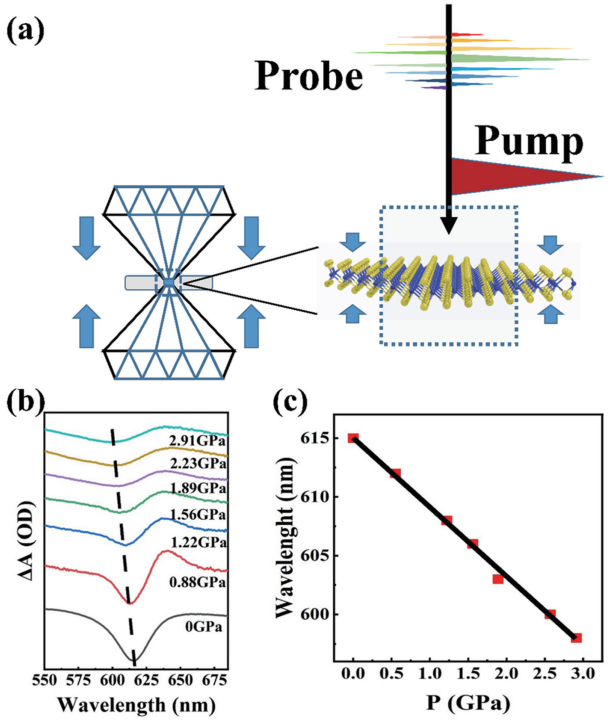

Fig. 5. (Color online) (a) Schematic of material structure and TA measurements of monolayer WS_2 in the DAC. (b) Evolution of TA spectra of monolayer WS_2 under pressure from 0.30 to 3.25 Gpa. (c) A exciton peaks as a function of pressures.

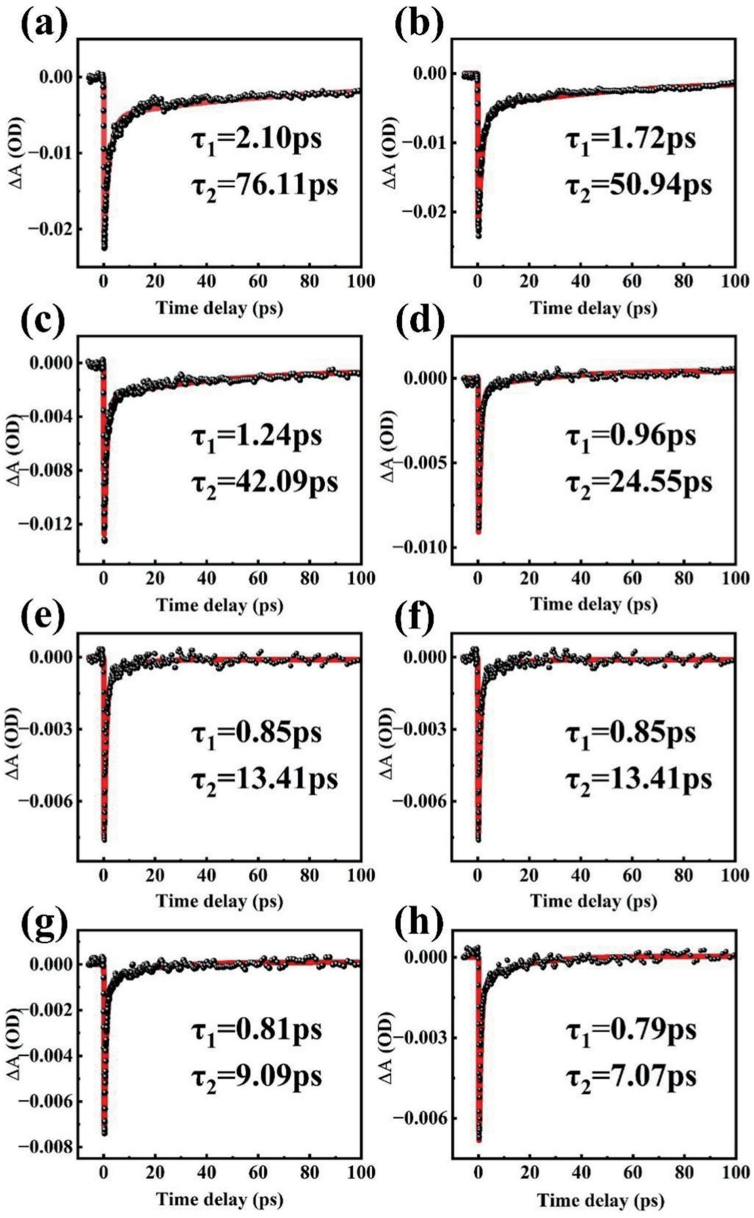

Fig. 6. (Color online) The transient absorption signals of monolayer WS_2 with different pressures: (a) 0.55 GPa; (b) 0.89 Gpa; (c) 1.22 Gpa; (d) 1.56 GPa; (e) 1.89 GPa; (f) 2.23 Gpa; (g) 2.56 Gpa; (h) 2.91 GPa. The red lines are fitting.

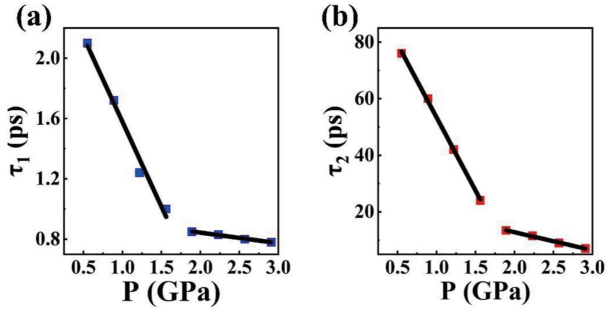

Fig. 7. (Color online) The time constants (a) τ_1 and (b) τ_2 of A exciton as a function of pressure.

slope variation of time constants upon compression, as shown in Fig. 7. For 0.55 GPa < P < 1.56 GPa, τ_1 changes with pressure at a rate of −1.12 ps/GPa and τ_2 declines with pressure at a rate of −51.78 ps/GPa. When the pressure is above 1.89 GPa, τ_1 shows a decline shift at a rate of −0.07 ps/GPa and that of τ_2 decreases to −6.38 ps/GPa.

For monolayer TMDs, the time constants τ_1 and τ_2 can be assigned to the carrier trapping process of the shallow and deep defect state with different capture rates. Considering the reduced dielectric screening effect and strong quantum confinement effect of TMDs, the Auger type dynamic process can be realized at low carrier densities. The τ_1 and τ_2 may be caused by Auger type carrier capture process of defect states, which means the electrons or holes in exciton states are captured by defect states by transferring the excess energy to other electrons and holes to satisfy the energy conservation law[29, 30]. According to this model, the quantum confinement effect may be enhanced by increasing the pressure, and the carriers are much easier to collide with other carriers. This feature means that the carriers are easier to release the excess energy to other electrons or holes, and this is beneficial for the Auger type carrier trapping process[31–33]. However, there is a different model that can explain the pressure-induced acceleration of the carrier cap-

ture process—the pressure can shorten the W–S bond in the monolayer WS_2, and enhance the vibration between W and S atoms, which can increase phonon energy and be confirmed by the above Raman results. This feature is conducive to meet the requirements of energy and momentum conservation in the capturing process[20, 21].

At around 1.56–1.89 GPa, a turning point appears and changes the time constants of two decay process with the decrease of pressure, which may result from the pressure induced changeover of the electronic structure. Both of the transient components are fully recovered when the pressure is released. Thus, the results clearly demonstrate that the band structure and carrier dynamics processes of monolayer WS_2 can be accurately manipulated by hydrostatic pressure.

4. Conclusions

In summary, we have synthesized a sample monolayer WS_2 to study the optical response of the sample with pressure via Raman spectroscopy and transient absorption spectroscopy. We found that hydrostatic pressure can be an efficient method to tune the lattice vibrations. The transition spectra were analyzed by tracking the energy shift and carrier dynamics of A exciton with different pressures. The results demonstrate the efficient tuning of band structure and photo-induced carrier recombination processes by pressure engineering. Our findings provide the basic information for understanding carrier dynamics in atomically thin TMDs under external strain.

Acknowledgements

This work was supported by Shenzhen Science and Technology Innovation Commission (JCYJ20220530153004010).

References

[1] Sharma I, Mehta B R. Enhanced charge separation at 2D MoS_2/ZnS heterojunction: KPFM based study of interface photovoltage. Appl Phys Lett, 2017, 110, 061602
[2] Ross R T, Nozik A J. Efficiency of hot-carrier solar energy converters. J Appl Phys, 1982, 53, 3813
[3] Liu H S, Han N N, Zhao J J. Atomistic insight into the oxidation of monolayer transition metal dichalcogenides: From structures to electronic properties. RSC Adv, 2015, 5, 17572
[4] Parzinger E, Miller B, Blaschke B, et al. Photocatalytic stability of single- and few-layer MoS_2. ACS Nano, 2015, 9, 11302
[5] Wang Q H, Kalantar-Zadeh K, Kis A, et al. Electronics and optoelectronics of two-dimensional transition metal dichalcogenides. Nat Nanotechnol, 2012, 7, 699
[6] Geim A K, Grigorieva I V. Van der Waals heterostructures. Nature, 2013, 499, 419
[7] Yin Z Y, Li H, Li H, et al. Single-layer MoS_2 phototransistors. ACS Nano, 2012, 6, 74
[8] Choi W, Cho M Y, Konar A, et al. High-detectivity multilayer MoS_2 phototransistors with spectral response from ultraviolet to infrared. Adv Mater, 2012, 24, 5832
[9] He Y M, Yang Y, Zhang Z H, et al. Strain-induced electronic structure changes in stacked van der Waals heterostructures. Nano Lett, 2016, 16, 3314
[10] Chen M, Xia J A, Zhou J D, et al. Ordered and atomically perfect fragmentation of layered transition metal dichalcogenides via mechanical instabilities. ACS Nano, 2017, 11, 9191
[11] Nayak A P, Yuan Z, Cao B X, et al. Pressure-modulated conductivity, carrier density, and mobility of multilayered tungsten disulfide. ACS Nano, 2015, 9, 9117
[12] Zhu Z Y, Cheng Y C, Schwingenschlögl U. Giant spin-orbit-induced spin splitting in two-dimensional transition-metal dichalcogenide semiconductors. Phys Rev B, 2011, 84, 153402
[13] Ye Z L, Cao T, O'Brien K, et al. Probing excitonic dark states in single-layer tungsten disulphide. Nature, 2014, 513, 214
[14] Selvi E, Ma Y Z, Aksoy R, et al. High pressure X-ray diffraction study of tungsten disulfide. J Phys Chem Solids, 2006, 67, 2183
[15] Hangyo M, Nakashima S I, Mitsuishi A. Raman spectroscopic studies of MX2-type layered compounds. Ferroelectrics, 1983, 52, 151
[16] Ramakrishna Matte H S S, Gomathi A, Manna A, et al. MoS_2 and WS_2 analogues of graphene. Angew Chem Int Ed, 2010, 49, 4059
[17] Duwal S, Yoo C S. Shear-induced isostructural phase transition and metallization of layered tungsten disulfide under nonhydrostatic compression. J Phys Chem C, 2016, 120, 5101
[18] Livneh T, Sterer E. Resonant Raman scattering at exciton states tuned by pressure and temperature in 2H-MoS_2. Phys Rev B, 2010, 81, 195209
[19] Nicolle J, Machon D, Poncharal P, et al. Pressure-mediated doping in graphene. Nano Lett, 2011, 11, 3564
[20] Cheng X R, Li Y Y, Shang J M, et al. Thickness-dependent phase transition and optical behavior of MoS_2 films under high pressure. Nano Res, 2018, 11, 855
[21] Chi Z H, Zhao X M, Zhang H D, et al. Pressure-induced metallization of molybdenum disulfide. Phys Rev Lett, 2014, 113, 036802
[22] Nayak A P, Pandey T, Voiry D, et al. Pressure-dependent optical and vibrational properties of monolayer molybdenum disulfide. Nano Lett, 2015, 15, 346
[23] Dou X M, Ding K, Jiang D S, et al. Tuning and identification of interband transitions in monolayer and bilayer molybdenum disulfide using hydrostatic pressure. ACS Nano, 2014, 8, 7458
[24] Li F F, Yan Y L, Han B, et al. Pressure confinement effect in MoS_2 monolayers. Nanoscale, 2015, 7, 9075
[25] Xia J, Yan J X, Wang Z H, et al. Strong coupling and pressure engineering in WSe2–MoSe2 heterobilayers. Nat Phys, 2020, 17, 92
[26] Wang H N, Zhang C J, Rana F. Ultrafast dynamics of defect-assisted electron–hole recombination in monolayer MoS_2. Nano Lett, 2015, 15, 339
[27] Cunningham P D, McCreary K M, Hanbicki A T, et al. Charge trapping and exciton dynamics in large-area CVD grown MoS_2. J Phys Chem C, 2016, 120, 5819
[28] Wang M S, Li W, Scarabelli L, et al. Plasmon-trion and plasmon-exciton resonance energy transfer from a single plasmonic nanoparticle to monolayer MoS_2. Nanoscale, 2017, 9, 13947
[29] Ruppert C, Chernikov A, Hill H M, et al. The role of electronic and phononic excitation in the optical response of monolayer WS_2 after ultrafast excitation. Nano Lett, 2017, 17, 644
[30] Li Y Z, Shi J A, Mi Y, et al. Ultrafast carrier dynamics in two-dimensional transition metal dichalcogenides. J Mater Chem C, 2019, 7, 4304
[31] Ahn C, Lim H. Synthesis of monolayer 2D MoS_2 quantum dots and nanomesh films by inorganic molecular chemical vapor deposition for quantum confinement effect control. Bull Korean Chem Soc, 2022, 43, 1184
[32] Sridevi R, Pravin J C, Babu A R, et al. Investigation of quantum confinement effects on molybdenum disulfide (MoS_2) based transistor using ritz Galerkin finite element technique. Silicon, 2022, 14, 2157
[33] Trovatello C, Katsch F, Li Q Y, et al. Disentangling many-body effects in the coherent optical response of 2D semiconductors. Nano Lett, 2022, 22, 5322

Yao Li is an M.S. student at the Shenzhen Technology University under the supervision of Prof. Haiou Zhu. His research focuses on the dynamic behavior of high-pressure carriers based on TMDs.

Zongpeng Song Zongpeng Song is an optical testing engineer in the analysis and testing center of Shenzhen Technology University. He received his Ph.D. degree in optical engineering from Shenzhen University. His research focuses on ultrafast spectroscopy.